Supporting Information (SI)

Electrosynthesis of poly(2,5-dimercapto-1,3,4-thiadiazole) films and their composites with gold nanoparticles at a polarised liquid|liquid interface

Marco F. Suárez-Herrera,[a, b,*] Alonso Gamero-Quijano[a,c,d] and Micheál D. Scanlon[a,c,e*]

[a] The Bernal Institute, University of Limerick (UL), Limerick V94 T9PX, Ireland.

[b] Departamento De Química, Facultad De Ciencias, Universidad Nacional De Colombia, Cra 30 # 45-03, Edificio 451, Bogotá, Colombia.

[c] Department of Chemical Sciences, School of Natural Sciences, University of Limerick (UL), Limerick V94 T9PX, Ireland.

[d] Department of Physical Chemistry, University of Alicante (UA), E-03080, Alicante, Spain.

[e] The Advanced Materials and Bioengineering Research (AMBER) Centre, CRANN Institute, Trinity College Dublin (TCD), Dublin 2 D02 PN40, Ireland.

E-mail: * mfsuarezh@unal.edu.co (M.F. Suárez-Herrera)

* micheal.scanlon@ul.ie (M.D. Scanlon)

ORCID IDs

Prof. Marco F. Suárez-Herrera: 0000-0002-7624-5982

Dr. Alonso Gamero-Quijano: 0000-0002-7173-2861

Dr. Micheál D. Scanlon: 0000-0001-7951-7085

S1. Experimental methods

S1.1. Chemicals. All chemicals were used as received without further purification. All aqueous solutions were prepared with ultrapure water (Millipore Milli-Q, specific resistivity 18.2 MΩ·cm). Bis(triphenylphosphoranylidene) ammonium chloride (BACl, 97%) and lithium tetrakis(pentafluorophenyl)borate diethyletherate ([Li(OEt$_2$)]TB) were obtained from Sigma-Aldrich and Boulder Scientific Company, respectively. Bis(triphenylphosphoranylidene)-ammonium tetrakis(pentafluorophenyl)borate (BATB) was prepared as reported elsewhere [1]. 1,3,4-thiadiazole-2,5-dithiol dipotassium salt (K_2DMcT) and 2,5-dimercapto-1,3,4-thiadiazole (H_2DMcT) were obtained from Sigma-Aldrich. Lithium chloride (LiCl, ≥95%), tetraethylammonium chloride (TEACl, ≥98%), lithium sulfate (Li_2SO_4, ≥98.5%), lithium iodide (LiI, 99.9%), iodine (I_2, 99.8%), mercury chloride ($HgCl_2$, ≥98.5%), phosphate buffered saline (PBS tablets), acetonitrile (≥98.5%), sulfuric acid (H_2SO_4, 95-98%) and PBS-stabilised 5 nm colloidal gold nanoparticle (AuNP) suspensions were obtained from Sigma-Aldrich. The organic solvent α,α,α-trifluorotoluene (TFT, 99%) was obtained from Acros Organics.

S1.2 Electrochemical measurements. Electrochemical experiments were carried out at an interface between two immiscible electrolyte solutions (ITIES) formed between water and α,α,α-trifluorotoluene using a four-electrode configuration (the geometric area of the cell was 1.60 cm^2). To supply the current flow, platinum counter electrodes were positioned in the organic and aqueous phases. The potential drop at the liquid|liquid (L|L) interface was measured by means of *pseud*o-reference silver/silver salt (Ag/AgX) electrodes, which were connected to the aqueous and organic phases, respectively, through Luggin capillaries (where X is the anion with the highest concentration in the aqueous phase, to ensure reference potential stability). The Galvani potential difference was attained by assuming the formal ion transfer potential of TMA^+ to be +0.311 V [2].

The general configurations of the electrochemical cells studied are outlined throughout the article, where each vertical line represents a phase boundary, and the double vertical line represents the polarisable L|L interface. Cyclic voltammograms (CVs) were measured using an Autolab PGSTAT204 potentiostat and a four-electrode electrochemical cell. The PGSTAT204 potentiostat was equipped with a frequency response analyser module (FRA32M) and differential capacitances at different applied voltages were measured by AC voltammetry at 80 Hz, as indicted, and assuming the cell behaves as a series R-C circuit.

S1.3 Simulations. CVs were simulated assuming a Frumkin isotherm as described in detail previously [3]. The kinetics were described by the Butler-Volmer equation and mass transport phenomena were neglected.

S1.4 Confocal Raman Spectroscopy. Raman spectroscopic measurements were performed using a LabRAM HR Evolution Raman Confocal Microscope (Horiba, France) with LabSpec 6 software. Measurements were performed with a 785 nm excitation laser source. Calibration was performed with a silicon standard (520.07 cm^{-1}). A long-distance ×50 objective with a numerical aperture of 0.85 and a working distance of 5 mm was used for all measurements. Final Raman spectra were typically obtained after averaging 10 individual spectra with 15 s of acquisition each. Gratins with 600 grooves·mm^{-1} for the 785 nm laser wavelength were used, leading to an average 1 cm^{-1} spectral resolution in the spectral range acquired.

S1.5 Scanning Electron Microscopy (SEM). SEM measurements were performed with a Hitachi SU-70 scanning electron microscope with 5 or 10 kV acceleration voltages in field immersion mode.

S2. Supplementary Figures

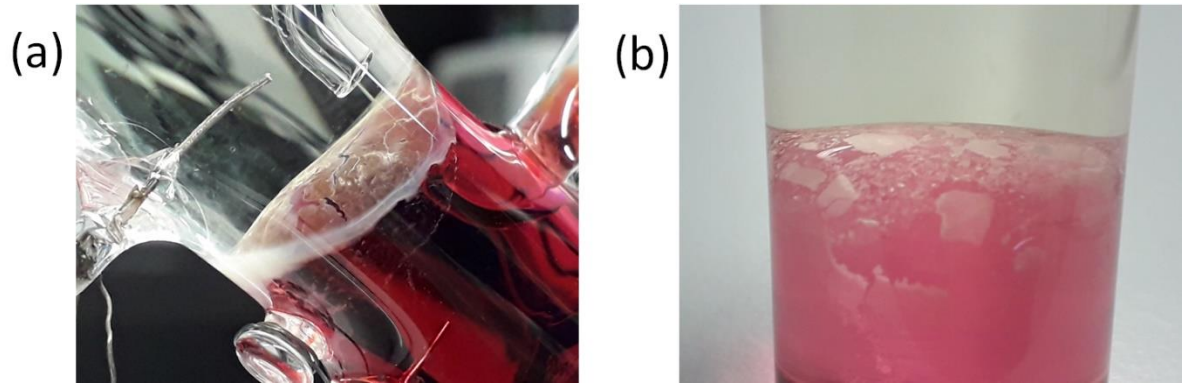

Figure S1. Optical images of poly(DMcT) electrosynthesised at a L|L interface were obtained using Electrochemical Cell 1 (see main text) under aerobic, ambient conditions with 5 mM K_2DMcT and 10 mM LiCl in the aqueous electrolyte and 5.7 mM organic I_2 **(a)** after 15 CV cycles with the potential window limited by switching currents set between +4 μA and –4 μA and **(b)** without external polarisation after 24 h.

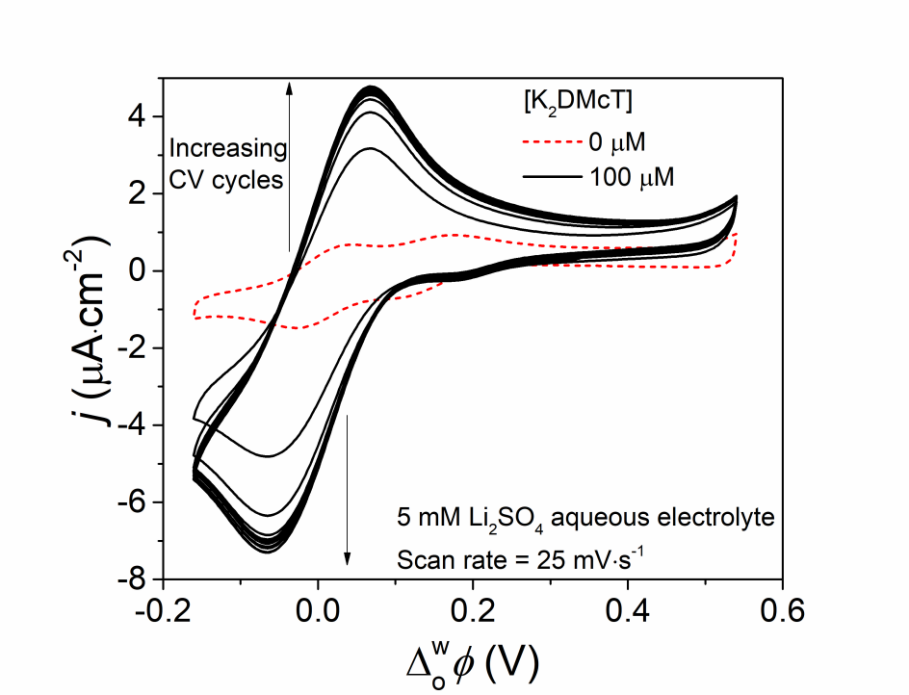

Figure S2. Repetitive CV cycles to electrosynthesis poly(DMcT) when the aqueous electrolyte was 5 mM Li_2SO_4 in the absence and presence of aqueous K_2DMcT. CV cycles 1 to 10 are shown. CVs were obtained at a scan rate of 25 mV·s^{-1}. Electrochemical experiments were carried out using Electrochemical Cell 1 (see main text) under aerobic, ambient conditions.

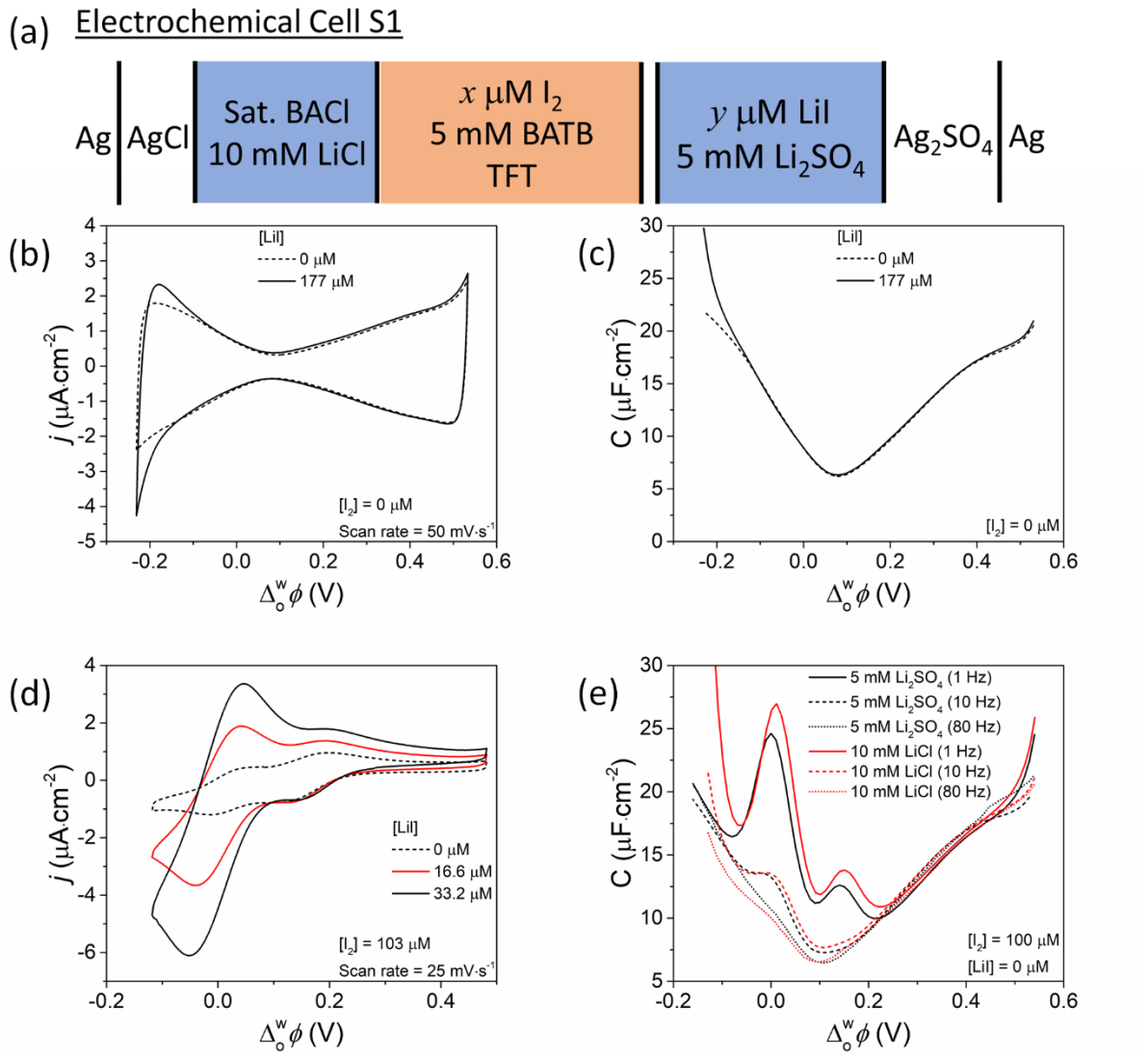

Figure S3. (a) Schematic representation of Electrochemical Cell S2 to produce I_3^- *in situ* at the polarised L|L interface (by the interfacial reaction of aqueous I^- and organic I_2) and monitor the reversible ion transfer behaviour of I_3^-. **(b)** CVs and **(c)** differential capacitance curves obtained in the absence and presence of 177 μM aqueous LiI, without I_2 dissolved in the organic phase. **(d)** CVs obtained in the absence and presence of 16.6 and 33.2 μM aqueous LiI, with 103 μM I_2 dissolved in the organic phase. CVs were obtained at scan rates of 25 or 50 $mV \cdot s^{-1}$ as indicated and differential capacitance curves were obtained using a voltage excitation frequency of 80 Hz. **(e)** The effect of applied voltage excitation frequencies of 1, 10 or 80 Hz on the AC voltammetry. Differential capacitance curves were obtained for 5 mM Li_2SO_4 and 10 mM LiCl aqueous electrolytes, respectively, in the absence of aqueous LiI and with 100 μM organic I_2. All electrochemical experiments were carried out using Electrochemical Cell S2 under aerobic, ambient conditions. With 10 mM LiCl in (e), the Ag/Ag_2SO_4 aqueous *pseudo*-reference electrode was replaced with a Ag/AgCl wire.

As organic I_2 was used to oxidise aqueous $DMcT^{2-}$, a series of control experiments involving Electrochemical Cell S1 (Fig. S3a) were designed to study the ion transfer properties of I^- and I^{3-}, both of which were expected to be generated at the ITIES during $DMcT^{2-}$ oxidation as described in Reactions (1) and (2) in the main text. Comparison of CVs obtained with and without aqueous LiI present (in the absence of organic I_2) demonstrated that the standard ion transfer potential of I^- lies beyond the negative limit of the polarisable potential window (PPW) (Fig. S3b). Differential capacitance curves show no shift of the potential of zero charge (PZC) in the presence of aqueous LiI (Fig. S3c), indicating that I^- does not adsorb at the L|L interface.

As described in Reaction (2) in the main text, I_2 reacts with I^- to form I_3^-. This reaction is important in many analytical applications and Fig. S3d clearly shows that I^- can be detected and quantified if I_2 is present in the organic phase. Two reversible diffusion-controlled charge transfer responses were observed with half-wave potentials within the available PPW at ca. 0 and +0.150 V, respectively (Fig. S2d). The charge transfer response at 0 V was attributed to the reversible ion transfer of I_3^- and that at +0.150 V was tentatively assigned to the reversible ion transfer of hypoiodite (IO^-), see Reaction (3) in the main text. These charge transfer responses both increased in magnitude when LiI was added to the aqueous phase. CVs obtained in the presence of organic I_2 but absence of aqueous LiI also show two low magnitude reversible diffusion-controlled charge transfer responses (Fig. S3d, dashed CV). These signals are due possibly to the presence of I^- and IO^- produced from the chemical reaction between I_2 and water, Reaction (3) of the main text. The I^- reacts with I_2 to form I_3^-, which is transferred at ca. 0 V.

The formation of I_3^- is greatly influenced by the polarity of the solvent. An increase in the formation constant of I_3^- was reported by Naorem *et al.* in mixtures of water and organic solvents, such as ethylene glycol, 2-methoxy ethanol and acetonitrile [4]. Therefore, the formation constant of I_3^-, including through the self-ionisation route, is likely to be higher at the L|L interface than in the bulk aqueous solution.

Differential capacitance curves were obtained with either 10 mM LiCl or 5 mM Li_2SO_4 aqueous electrolytes in the presence of I_2 and absence of LiI (Fig. S3e). Some I_3^- was still generated in these experiments as described above, leading to the observation of two peaks (Fig. S3e). The most appropriate frequency to study the interfacial capacitance using AC voltammetry without the interference of the ion transfer of I_3^- was identified as 80 Hz, irrespective of the aqueous electrolyte used. This observation is in line with our previous work,

where we modulated the intensity of the Faradaic response due to ion transfer of tetraalkyammonium cations by changing the voltage excitation frequency during AC voltammetry [5]. As ion transfer is a diffusion-limited process, the intensity of the Faradaic response is low at 80 Hz, and this frequency can be chosen to measure the differential capacitance with good accuracy even in the presence of I_3^- anions (Fig. S3e). However, at a lower frequency of 1 Hz, the longer time frame of voltage excitation enhances the reversible Faradaic I_3^- ion transfer signal (Fig. S3e).

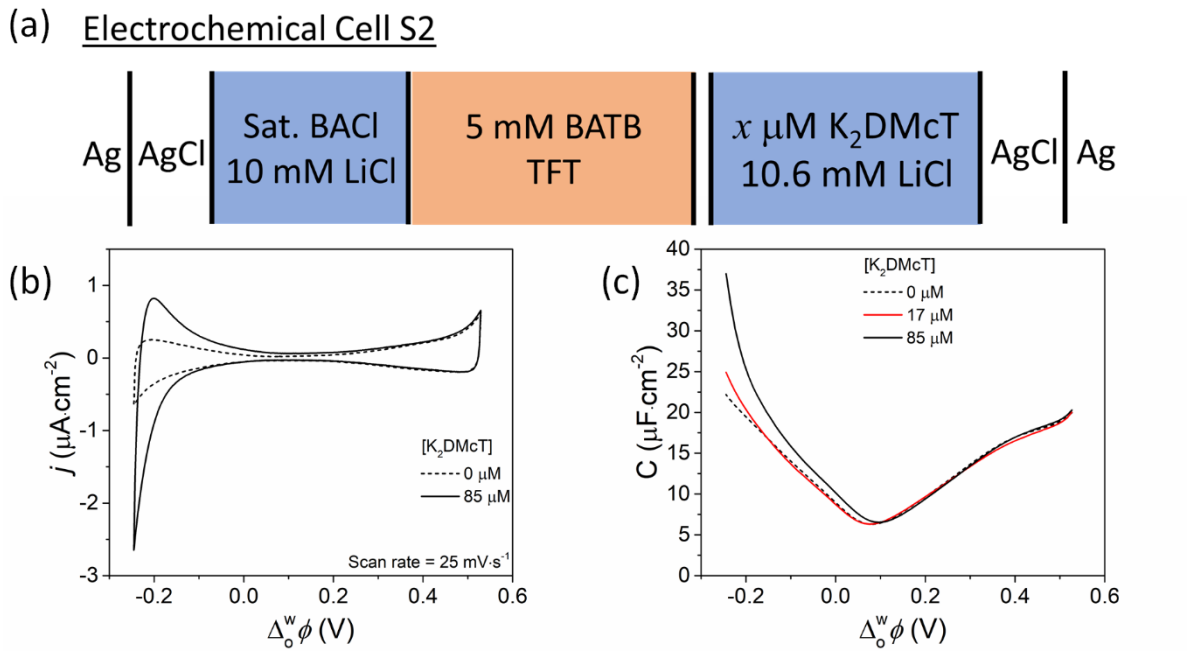

Figure S4. (a) Schematic representation of Electrochemical Cell S2 to observe the influence of the presence of aqueous K_2DMcT on electrochemical measurements at a polarised L|L interface. **(b)** CVs obtained in the absence and presence of 85 μM aqueous K_2DMcT. CVs were obtained at a scan rate of 25 mV·s^{-1}. **(c)** Differential capacitance curves obtained in the absence and presence of 17 and 85 μM aqueous K_2DMcT using a voltage excitation frequency of 10 Hz. All electrochemical experiments were carried out using Electrochemical Cell S2 under aerobic, ambient conditions.

CVs and differential capacitance curves were obtained for Electrochemical Cell S2 (Fig. S4a) with $DMcT^{2-}$ dissolved in the aqueous phase. Comparison with the CV in the absence of $DMcT^{2-}$ clearly shows that the standard ion transfer potential of $DMcT^{2-}$ lies beyond the negative limit of the (PPW) at the ITIES (Fig. S4b). An increase in negative current at negative potentials does, however, show that $DMcT^{2-}$ transfers more easily that the Cl^- aqueous electrolyte anion to the organic phase. Differential capacitance curves show a progressive shift of the PZC to positive potentials in the presence of increasing concentrations of $DMcT^{2-}$ (Fig. S4c), indicating that $DMcT^{2-}$ adsorbs at the L|L interface.

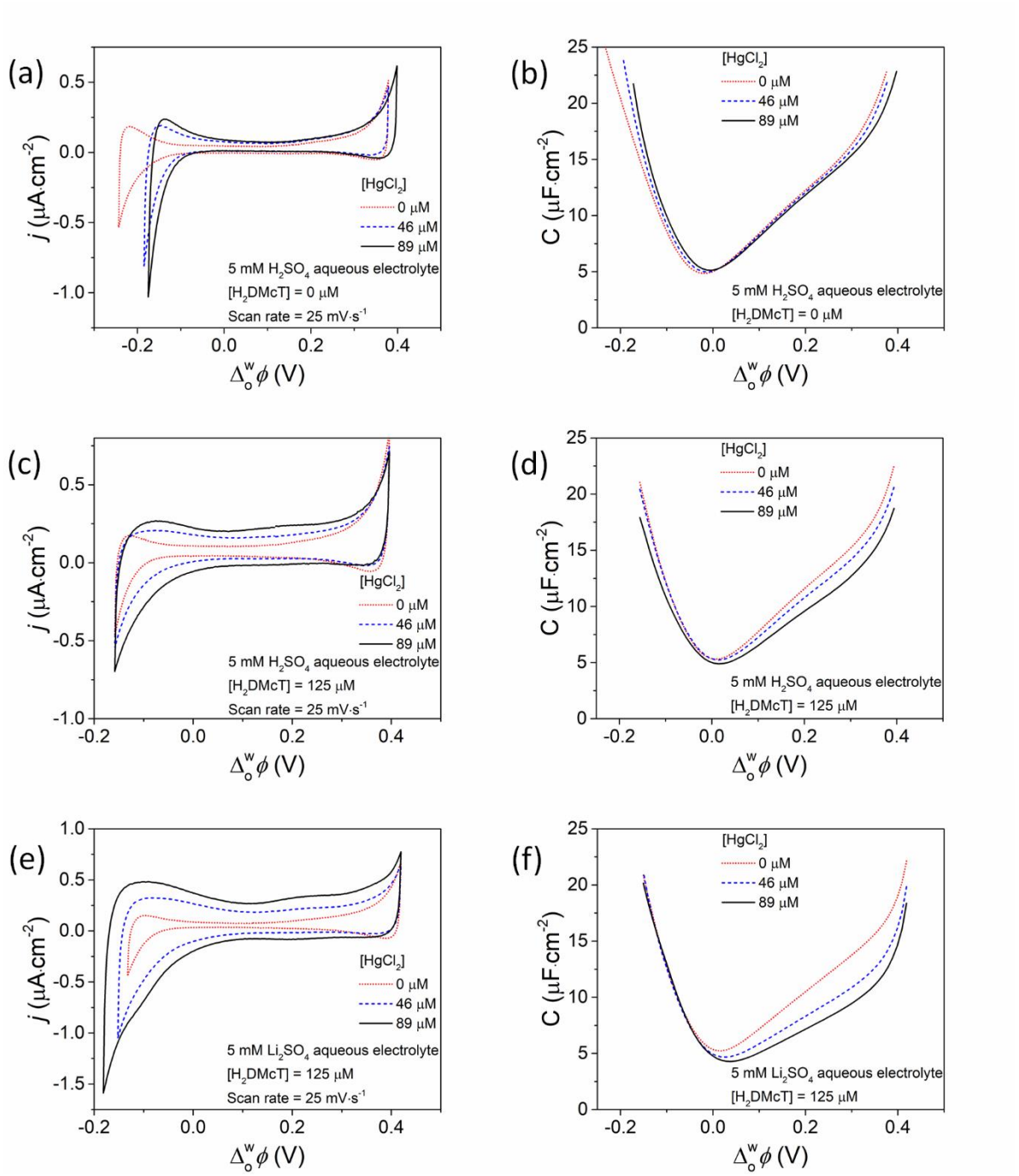

Figure S5. CVs and differential capacitance curves obtained in the absence and presence of increasing concentrations of aqueous $HgCl_2$ **(a, b)** with 5 mM H_2SO_4 aqueous electrolyte and 0 μM organic H_2DMcT, **(c, d)** with 5 mM H_2SO_4 aqueous electrolyte and 125 μM organic H_2DMcT, and **(e, f)** with 5 mM Li_2SO_4 aqueous electrolyte and 125 μM organic H_2DMcT. CVs were obtained at a scan rate of 25 mV·s^{-1}. CVs shown were for CV cycle 50 with H_2SO_4 and Li_2SO_4 aqueous electrolytes. Differential capacitance measurements were taken using a voltage excitation frequency of 10 Hz after 5 CV cycles (at 25 mV·s^{-1}) with LiCl aqueous electrolyte and 50 CV cycles (at 25 mV·s^{-1}) with H_2SO_4 and Li_2SO_4 aqueous electrolytes. All

electrochemical experiments were carried out using Electrochemical Cell 2 (see main text) under aerobic, ambient conditions.

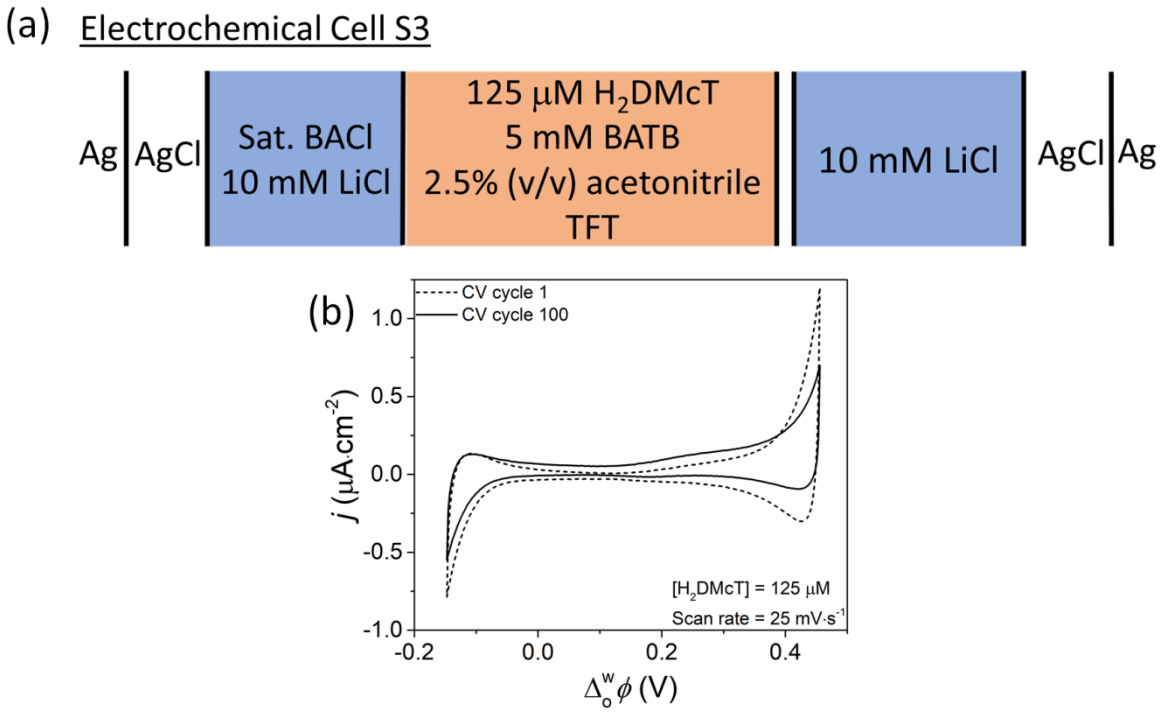

Figure S6. (a) Schematic representation of Electrochemical Cell S3 to explore the oxidation of organic solubilised H_2DMcT by O_2 (dissolved in both the aqueous and organic phases) in the absence of an electrocatalyst at a polarised L|L interface. **(b)** Comparison of CV cycles 1 and 100 obtained at a scan rate of 25 mV·s^{-1} using Electrochemical Cell S3 under aerobic, ambient conditions.

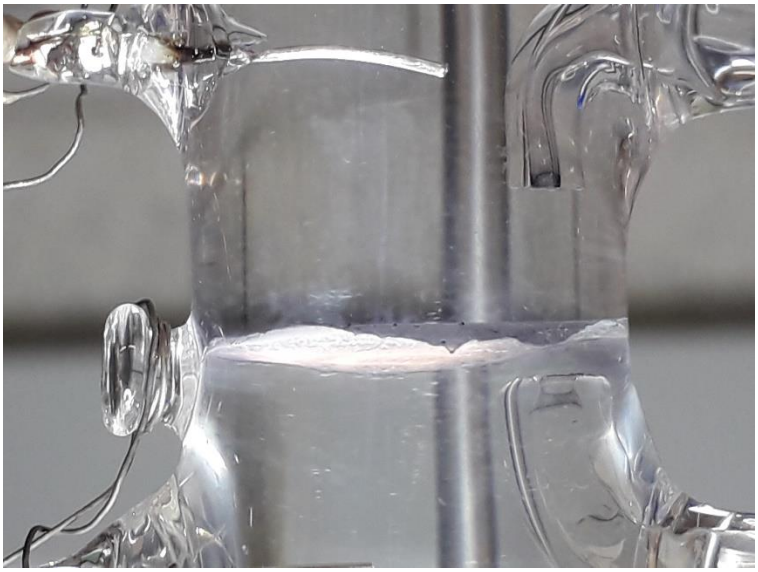

Figure S7. Optical image of the white underside (or organic-facing side) of a free-floating AuNP/poly(DMcT) interfacial film after all remaining colloidal AuNPs in the bulk aqueous phase were extracted by thoroughly rinsing with a colloidal AuNP-free aqueous electrolyte solution (*e.g.*, 10 mM LiCl).

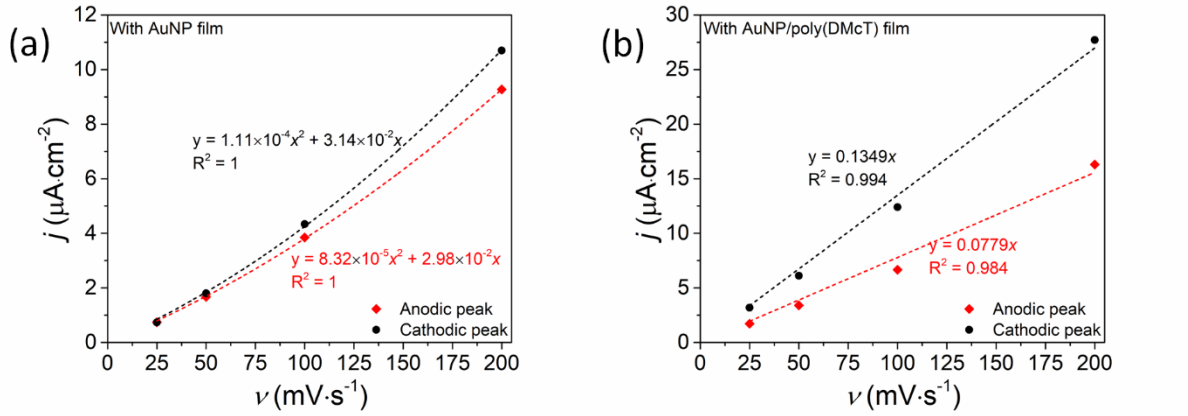

Figure S8. Comparison of peak height, j ($\mu A \cdot cm^{-2}$), *versus* scan rate, ν ($mV \cdot s^{-1}$), for the CVs shown in Figures 5(c) and (d) obtained using Electrochemical Cells 5a and 5b, respectively (see main text) with a AuNP interfacial film and AuNP/poly(DMcT) film at the L|L interface, respectively.

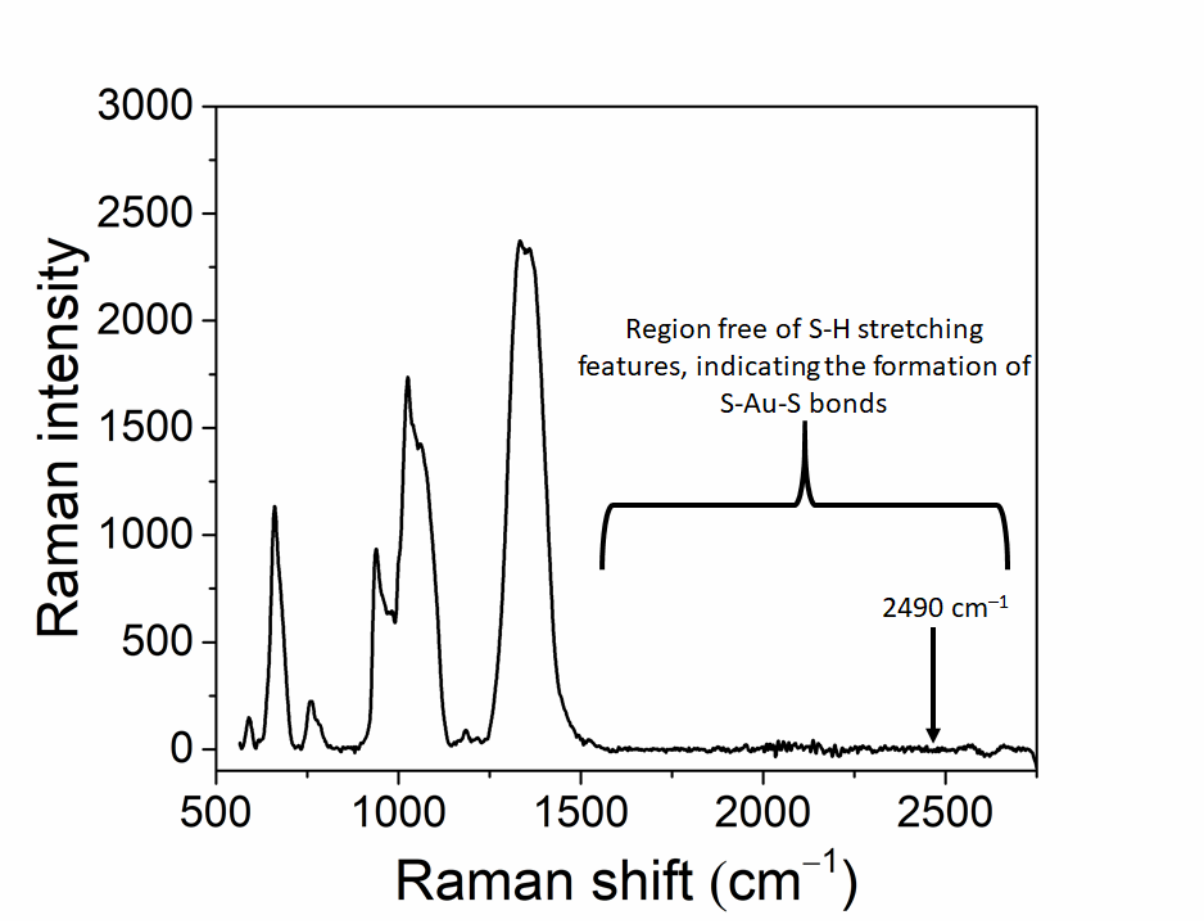

Figure S9. Raman spectrum of a AuNP/poly(DMcT) film immobilised on a silicon wafer displaying a wider Raman vibrational frequency range (500 to 2500 cm^{-1}). The excitation laser wavelength was 785 nm.

S3. Supplementary References

[1] M.F. Suárez-Herrera, M.D. Scanlon, On the non-ideal behaviour of polarised liquid-liquid interfaces, Electrochim. Acta. 328 (2019) 135110. https://doi.org/10.1016/j.electacta.2019.135110.

[2] E. Smirnov, P. Peljo, M.D. Scanlon, H.H. Girault, Gold Nanofilm Redox Catalysis for Oxygen Reduction at Soft Interfaces, Electrochim. Acta. 197 (2016) 362–373. https://doi.org/10.1016/j.electacta.2015.10.104.

[3] M.F. Suárez-Herrera, A. Gamero-Quijano, J. Solla-Gullón, M.D. Scanlon, Mimicking the microbial oxidation of elemental sulfur with a biphasic electrochemical cell, Electrochim. Acta. 401 (2022) 139443. https://doi.org/10.1016/j.electacta.2021.139443.

[4] H. Naorem, S.D. Devi, Spectrophotometric determination of the formation constant of triiodide ions in aqueous-organic solvent or polymer mixed media both in absence and presence of a surfactant, Spectrochim. Acta - Part A Mol. Biomol. Spectrosc. 101 (2013) 67–73. https://doi.org/10.1016/j.saa.2012.09.058.

[5] M.F. Suárez-Herrera, M.D. Scanlon, Quantitative Analysis of Redox-Inactive Ions by AC Voltammetry at a Polarized Interface between Two Immiscible Electrolyte Solutions, Anal. Chem. 92 (2020) 10521–10530. https://doi.org/10.1021/acs.analchem.0c01340.